

The relative roles of divergence and velocity slip in the stability of plane channel flow

K.C. Sahu¹, A. Sameen^{2,a}, and R. Govindarajan³

¹ Department of Chemical Engg., Imperial College, UK

² International Centre for Theoretical Physics, Trieste 34014, Italy

³ Engineering Mechanics Unit, Jawaharlal Nehru Centre for Advanced Scientific Research, Bangalore 560 064, India

Received: 21 January 2008 / Received in final form: 23 May 2008 / Accepted: 6 June 2008
Published online: 6 August 2008 – © EDP Sciences

Abstract. Wall slip and wall divergence are known to have large and opposing effects on the stability of flow in a two-dimensional channel. While divergence hugely destabilises, slip dramatically stabilizes the linear mode. In a non-parallel stability analysis, we study a combination of these two effects, since both will coexist in small-scale flows with wall roughness. Our main results are (i) that the stabilising effect of slip is reversed at higher angles of divergence, (ii) transient growth of disturbances is unaffected by either wall-divergence, or by slip at any divergence. Moreover, at the Reynolds numbers relevant here, transient growth is too low to be a significant player in transition to turbulence, which is more likely to be driven by linear instability. The results would have implications for the onset of unsteadiness and mixing in small scale flows.

PACS. 47.20.-k Flow instabilities – 47.15.Fe Stability of laminar flows – 47.27.nd Channel flow

1 Introduction

Chaotic advection and mixing in small scale flows are desirable features in several biological and chemical applications. Such mixing is usually achieved by constructing a convoluted flow chamber with a carefully designed system of vanes. It is assumed, and usually true, that such mixing is impossible at low Reynolds numbers in a simple geometry. In a straight channel, for example, laminar flow is linearly stable up to a Reynolds number of 5772, based on the channel half-width and the centreline velocity. Although the flow goes to turbulence at a Reynolds number far lower, between 1000 and 2000, (we will return soon to this) the value is probably too large to be of significance in small-scale flows. Moreover, in small scale applications, we may expect a significant velocity slip at the wall, which has been shown recently to push up the instability Reynolds number to huge values in a straight channel [1–3]. On the other hand, when there is no slip, but the walls are divergent rather than straight, the instability critical Reynolds number is well-known to plummet by orders of magnitude for even a small divergence [4,5]. We investigate here the combination of channel divergence and wall-slip, two large and opposing contributors to stability. Our motivation is that in small-scale flows, wall-roughness can create local divergence and convergence of the flow, and slip can be significant, especially if the walls are hydrophobic, so the

two effects are likely to act simultaneously. We find that wall slip has a destabilising effect (although small) in divergent flows, rather than the expected huge stabilization.

In the straight channel or in a pipe, the mechanisms leading to turbulence below the critical Reynolds number (for linear instability) are accepted to be either directly nonlinear, or triggered initially by transient algebraic growth due to the superposition of linearly decaying waves. In the latter case, nonlinearities are said to take over once transient growth increases disturbance amplitudes to significant levels. Transient growth of instabilities have been shown [1] to be not affected much by velocity slip at the wall for a straight channel, but have not been investigated before in a divergent channel, to our knowledge, with or without slip.

Our main results are as follows. Under no-slip condition at the wall, our non-parallel linear stability analysis, confirms the result obtained by [4] under the parallel flow assumption, that with increase in divergence, the critical Reynolds numbers falls sharply. The fact that the flow is non-parallel, namely that the basic flow is a function of the downstream coordinate as well as the wall-normal one, has only a small quantitative contribution. This is unlike a divergent pipe, where the effect was large [6]. We show that transient growth of disturbances, on the other hand, is unaffected by wall divergence. At the relevant Reynolds numbers, the magnitude of maximum of transient growth is small, so linear instability leading to exponential growth

^a e-mail: asameen@ictp.it

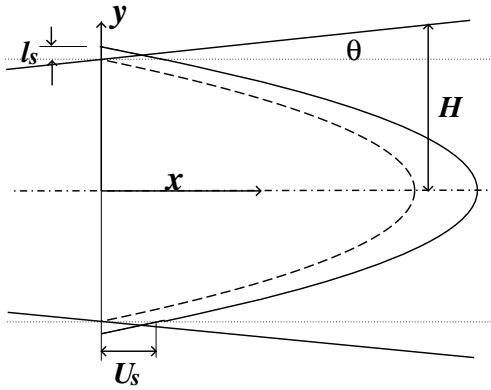


Fig. 1. A schematic diagram showing the coordinate system, slip length and slip velocity.

of disturbance is expected to be the major player in these flows. As mentioned before, slip at the walls does not in this case have the “obvious” effect of huge stabilisation. In fact, wall slip can further destabilise the flow, although slightly. While the present “weakly non-parallel” [6] approach is appropriate for small angles of divergence, we are working on a full two dimensional eigenvalue solver for the stability of slipping flow through arbitrary geometries.

At low Knudsen numbers, we take the Navier-Stokes equations to be valid in conjunction with the slip boundary condition of Maxwell [7],

$$U \pm Kn \frac{dU}{dy} = 0, \quad \text{at } y = \pm 1. \quad (1)$$

Through out this paper U , V , W denote base velocities and u , v , w are the perturbation velocities in the streamwise, (x), normal, (y) and spanwise, (z) directions respectively. This model is correct to $O(1)$ in the Knudsen number, Kn , expressed here as the ratio of slip length (l_s) to the local half-width $H(x)$ of the channel. All quantities are non-dimensionalised using $H(x)$ and the centreline velocity $U_c(x)$. In particular, the relationship $dx_d = H dx$ is used later, where the subscript d represents a dimensional quantity. The Maxwell slip model breaks down around $Kn = 0.15$ [8], so we, like others [1–3,9] who use this model, restrict ourselves to values below this. The slip length and slip velocity (U_s) are shown schematically in Figure 1.

Incidentally the work of Lauga & Cossu [1] set to rest a recent controversy over the effect of slip on the stability of channel flow. Chu [9–11] had found a large destabilisation due to slip, in contrast to the earlier prediction of Gersting [12] of a huge stabilisation. The conclusions of [12] are confirmed by [1], who showed that there was a lapse in the application of the slip boundary condition in the work of Chu. There remains a small discrepancy in the effect of slip on transient growth, between the results of [1,2]. Both agree that the effect of slip is small, but the direction of the effect is stabilising in [2] and destabilising in the other. We have checked that this discrepancy arises from a difference in the definition of Reynolds number, since

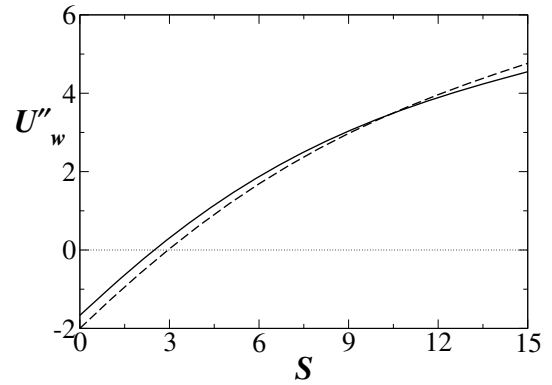


Fig. 2. Variation of U'' at the wall for different S (solid line: $Kn = 0.1$ and dashed line: $Kn = 0$).

the velocity scale (from their respective analytical expressions) used by [2] decreases with increasing slip while that of [1] goes up with slip. In the present paper we avoid this ambiguity by scaling with the centreline velocity, obtained numerically, as explained in the next section. For the sake of validating our results, when we employ the respective definitions of [1,2], our calculations for a plane channel agree very well with each.

For a divergent channel, we use the Jeffery-Hamel mean flow profiles, described in the next section, followed in subsequent sections by the linear stability and computations of transient disturbance growth.

2 The basic flow

At low angles of divergence, the incompressible laminar flow in a wedge-shaped channel is given by the Jeffery-Hamel equation (see e.g. [4]):

$$U''' + 2SUU' = 0, \quad (2)$$

which is valid for flows with slip boundary conditions as well. All effects up to the first order in the divergence have been retained in the Navier-Stokes equations, and similarity has been assumed. The primes denote derivative with respect to y . The only parameter is the product $S \equiv aRe$, of the slope a of the wall and the Reynolds number Re . (Some of the results below are presented in terms of the angle of divergence $\theta = \tan^{-1} a$). From global continuity we see that $Re \equiv H(x)U_c(x)/\nu$ is a constant for a given flow, ν being the kinematic viscosity. The normal velocity

$$V = ayU \quad (3)$$

from continuity. Note that V , being normal to the centreline, is not zero at the wall when there is a non-zero slip (U_s). Equation (3) with the boundary conditions given by equation (1) at the wall, and $U = 1$, $U' = 0$ at the centreline, is solved by a fourth order Runge-Kutta method. Thus for different Knudsen number the profile is computed numerically. The effect of slip at different S on the streamwise and normal components of the velocity is shown in Figures 3 and 4 respectively.

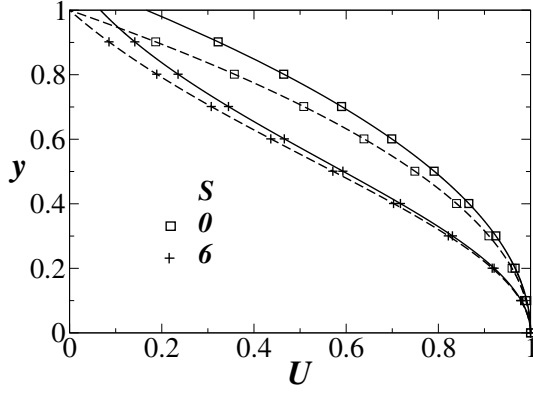


Fig. 3. Streamwise components of the velocity at various values of the divergence parameter S . Solid line: $Kn = 0.1$, dashed line: no slip. The U and V are symmetric and anti-symmetric about the channel centreline ($y = 0$) respectively.

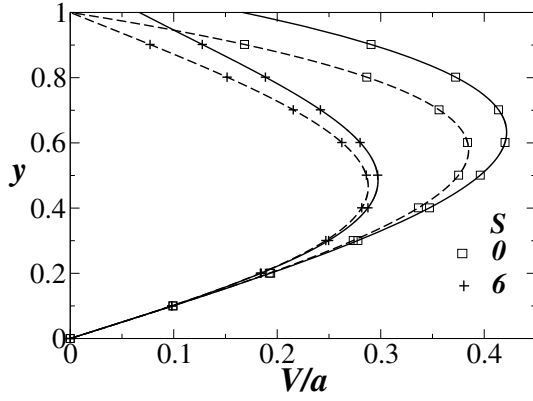


Fig. 4. Normal, components of the velocity at various values of the divergence parameter S . Solid line: $Kn = 0.1$, dashed line: no slip. The U and V are symmetric and anti-symmetric about the channel centreline ($y = 0$) respectively.

Ever since Rayleigh [13] proved that a point of inflexion in the velocity profile is a necessary condition for inviscid instability, the second derivative U'' has been known to be a sensitive indicator of linear instability, especially when it goes through a zero somewhere in the flow. In a divergent channel, U'' at the centreline remains negative, and for small divergences, is close to the value in a plane channel of -2 . The dependence of U'' at the wall on S is shown in Figure 2. A positive value is indicative of the existence of an inflexion point. In the absence of slip, the profile is inflexional beyond $S = 2.95$, whereas for $Kn = 0.1$, the profile is inflexional for $S \geq 2.5$. Going by this inviscid argument, a divergent channel might be expected to be more unstable with slip than without, but the difference is too small to predict the direction of the effect at finite Reynolds numbers. We may however estimate that for a profile that is near-inflexional, the divergence could be more important for stability than changes in the boundary conditions. In the next section, we will investigate if the above argument is correct with a non-parallel linear stability analysis.

3 Non-parallel stability analysis

We consider small divergence angles and Reynolds numbers are much larger than 1, so streamwise variations in the basic flow are slow. A consistent non-parallel approximation is to retain all terms up to $O(a)$ and $O(Re^{-1})$ and to neglect terms of higher order in either of these. As in parallel stability analysis [14], each flow quantity is expressed as the sum of a steady mean and a time-dependent perturbation, such as

$$u = U(y) + \hat{u}(x, y, z, t). \quad (4)$$

Note that, y being the similarity variable, the basic velocity in equation (4) is a function of y alone. Our numerical results for non-similar velocity profiles show that $U = U(y)$ is a fair assumption whenever $\partial U/\partial x$ is smaller than the inverse of the Reynolds number. The dependence on the streamwise coordinate may be expressed as the product of a rapidly varying wave-like part scaled by a relatively slowly varying function (see e.g. [6,15]), and normal modes may be used in the spanwise coordinate z and in time, as

$$[\hat{u}] = \text{Real} \left\{ u(x, y) \exp \left(i \left(\int \alpha(x) dx + \beta z - \omega t \right) \right) \right\}, \quad (5)$$

such that $\partial u/\partial x \sim O(Re^{-1})$. The streamwise and spanwise wavenumbers are α and β respectively and ω is the disturbance frequency. Flow quantities of the form (4) are substituted in the Navier-Stokes and continuity equations. The mean flow is subtracted out, and the nonlinear terms in the perturbations are neglected. Since the divergence angle is small and the Reynolds number is large, we retain all terms up to and including $O(a)$ and $O(1/Re)$ and neglect all terms of higher order. We thus obtain the non-parallel linear stability equations, for the diverging channel. Note that both the base state and the stability equations are correct up to the same order, i.e., the first term neglected in each is $O(a)$ and $O(1/Re)$. The equations for linear stability under these assumptions are (for details Refs. [6,16]),

$$-au + \frac{\partial u}{\partial x} + i\alpha u - ay \frac{\partial u}{\partial y} + \frac{\partial v}{\partial y} + i\beta w = 0, \quad (6)$$

$$i(\alpha U - \omega)u + U \left[\frac{\partial u}{\partial x} - 2au \right] + (v - ayu)U' = \quad (7)$$

$$-\frac{\partial p}{\partial x} + (2a - i\alpha)p + ay \frac{\partial p}{\partial y} + \frac{1}{Re} \left[\frac{\partial^2 u}{\partial y^2} - (\alpha^2 + \beta^2)u \right],$$

$$i(\alpha U - \omega)v + U \frac{\partial v}{\partial x} + ayU'v = -\frac{\partial p}{\partial y} + \frac{1}{Re} \quad (8)$$

$$\times \left[\frac{\partial^2 v}{\partial y^2} - (\alpha^2 + \beta^2)v \right],$$

$$i(\alpha U - \omega)w + U \frac{\partial w}{\partial x} = -i\beta p + \frac{1}{Re} \left[\frac{\partial^2 w}{\partial y^2} - (\alpha^2 + \beta^2)w \right]. \quad (9)$$

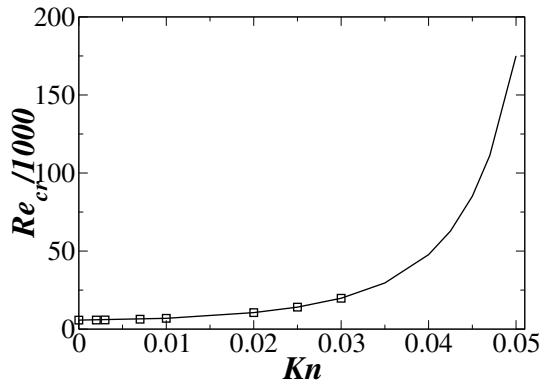


Fig. 5. Variation with velocity slip at the wall of the critical Reynolds number Re_{cr} for linear instability in a plane channel. Line: present study, symbols: [1].

The boundary conditions are

$$u \pm Kn \frac{\partial u}{\partial y} = v \mp au = w \pm Kn \frac{\partial w}{\partial y} = 0 \quad \text{at } y = \pm 1, \quad (10)$$

with finite pressure at the walls. In equations (6) to (10), if we set a , and all the streamwise derivative terms to zero, and substituting $\eta = i\beta u - i\alpha w$, we obtain the Orr-Sommerfeld and Squire equations for parallel flow [14].

We solve equations (6–10) by the method described in detail in [6]. Briefly, the idea is to pose an eigenvalue problem of twice the dimensions as the number of grid points to account for the coupling of two neighbouring streamwise locations. This is made possible upon discretising the streamwise derivative and using the fact that the dimensional frequency remains constant downstream. We use Chebyshev collocation spectral discretisation. We always find that the even mode in v is much more unstable than the odd mode. When appropriate, this fact is used to speed up the computations by considering only a half-channel.

While Squire's theorem is not applicable directly for non-parallel flows, it is usually the case that two-dimensional perturbations are the least stable in flows which vary slowly in x . This is true in the case of divergent channels too [16], so only two-dimensional perturbations are presented in this section on linear instability. The two parameters in the problem under consideration are channel divergence and wall slip. For a plane channel ($\theta = 0$), the present solutions match well with [1] as seen in Figure 5. It is seen that the critical Reynolds number increases sharply with increase in the Knudsen number (nearly 175% for a Knudsen number rise of 0.05). For different wall divergence the same variation is given in next two figures as neutral stability curves. The boundaries of neutral stability at various Knudsen number for angles of divergence $\theta = 0.1^\circ$ and 1° are shown in Figures 6 and 7 respectively. At the lower level of divergence, slip is seen to stabilise the flow, but much less than it would in a plane channel, only $\sim 22\%$ for an angle of 0.1° , Figure 6. At the larger divergence, increasing the Knudsen number has a small destabilising effect only $\sim 10\%$ for an angle of 1° , Figure 7. The effect of slip and divergence is summarised

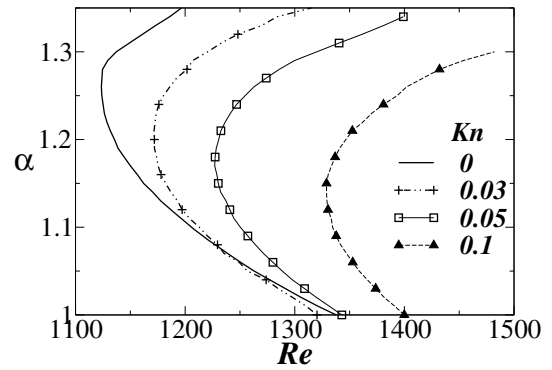


Fig. 6. Neutral stability curve for different values of Kn , angle of divergence = 0.1° .

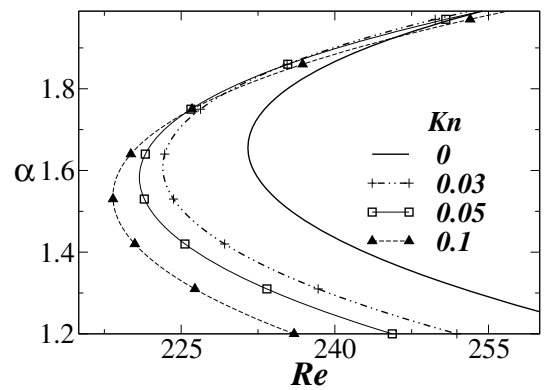


Fig. 7. Neutral stability curve for different values of Kn , angle of divergence = 1° .

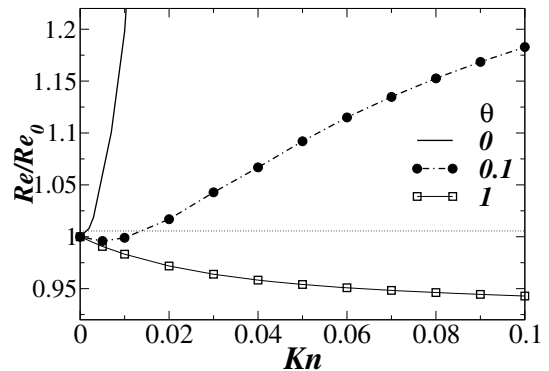


Fig. 8. Re/Re_0 vs. Kn for different angle of divergence (θ).

in the plot of the critical Reynolds number Re_{cr} in Figure 8. To highlight the result, we plot Re_{cr}/Re_0 vs. Kn , where Re_0 is the critical Reynolds number for the no-slip ($Kn = 0$) case. As the angle of divergence increases, the effect of slip is progressively reversed, from being hugely stabilising to mildly destabilising.

Figure 9 shows the cross-over in the critical Reynolds number. Figure 10 a portion of the figure is magnified and compared with [5]. At a Knudsen number of 0.1, Re_{cr} varies with wall slope approximately as a power law, with an exponent of -0.8 . This means that the parameter S at which the flow is neutrally stable increases slowly with the wall slope, roughly as $S \sim a^{0.2}$. It is worth noting

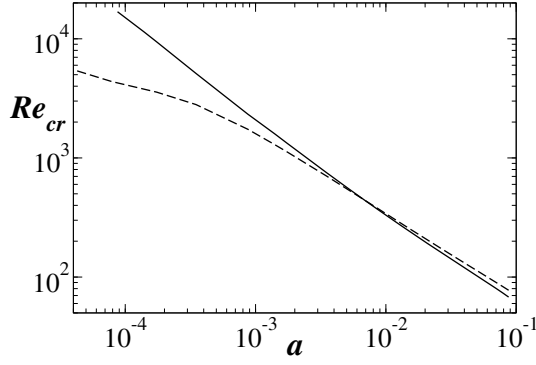


Fig. 9. Variation of the critical Reynolds number, Re_{cr} with wall divergence, solid line: $Kn = 0.1$, dashed line: $Kn = 0$.

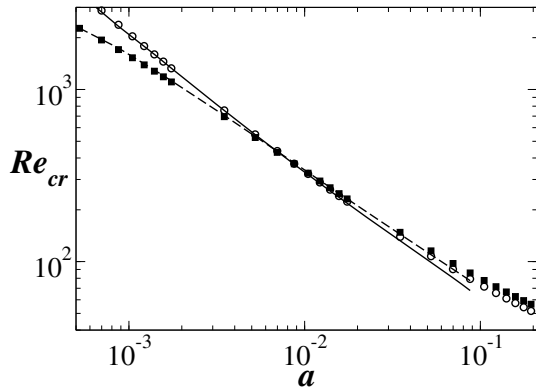


Fig. 10. A portion of Figure 9 is magnified, with the corresponding results from the Orr-Sommerfeld equation [4] shown in symbols.

that as S increases, the slope of the velocity profile at the wall decreases, so a given Knudsen number corresponds to smaller slip velocities at higher divergences. The results from the Orr-Sommerfeld equation applied to the Jeffery-Hamel profiles are shown in the same figure. It may be concluded that for wall divergences below a degree, flow non-parallelism acts only through the basic profile, and the explicit non-parallel terms (terms containing a and partial derivatives of u, v, w and p in x , in Eqs. (6–9)) are negligible. This has been checked to be true for the entire spectrum of eigenvalues for a variety of conditions. Beyond this angle, explicit non-parallel effects are noticeable but not large. At the largest divergences shown, i.e., for $a \sim 0.2$, the flow is mildly separated at the critical Reynolds number. Any firm statements at these angles of divergence would require a non-parallel stability analysis correct to a higher order of accuracy in a and $O(Re^{-1})$ than considered here. We only show Orr-Sommerfeld results as a qualitative indicator that nothing special happens when one encounters a mildly separated profile.

4 Transient growth

In contrast to the least stable linear eigenmode, the maximum transient growth of disturbance kinetic energy is

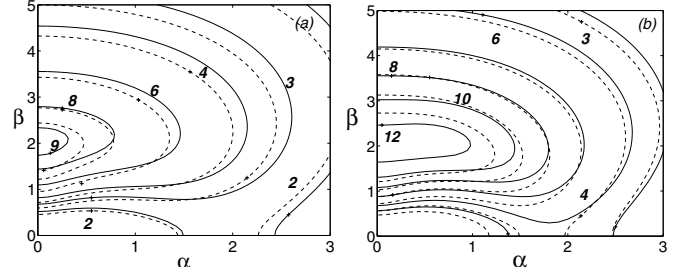


Fig. 11. The contour of G_{max} for $Re = 200$ without slip (solid lines) and at $Kn = 0.1$ (dashed lines) for (a) $a = 0.005$, and (b) $a = 0.02$. At the latter wall divergence, a Reynolds number of 200 is 95% of the critical Re for linear instability.

shown here to depend primarily on the Reynolds number of the flow and not on the slope of the walls. The introduction of velocity slip at the walls has a very small effect in the presence of divergence as well, similar to the findings for a plane channel of [1,2]. While the linear stability computations use a full non-parallel analysis, we found that the spectrum was not too sensitive to the extra accuracy afforded by the non-parallel terms. Given the negligible effect of the non-parallel terms on the stability, we use eigenvalues and eigenfunctions from the Orr-Sommerfeld and Squire equations with slip boundary conditions. The equation (5) is thus of the form,

$$[\hat{u}] = \text{Real} \{u(y) \exp(i(\alpha x + \beta z - \omega t))\}. \quad (11)$$

If $\Lambda = \text{diag}\{\omega_1, \omega_2, \dots, \omega_N\}$ is constructed out of the N least stable eigenvalues of this system, and κ is similarly constructed from the expansion coefficients of the corresponding eigenfunctions, the resulting disturbance kinetic energy, $g(t)$, may be written as [17]

$$g(t) = \frac{\|\kappa(t)\|_E^2}{\|\kappa(0)\|_E^2} = \frac{\|e^{-i\Lambda t} \kappa(0)\|_E^2}{\|\kappa(0)\|_E^2}. \quad (12)$$

Maximising $g(t)$ for all possible initial conditions $\kappa(0)$, we define

$$G(t) \equiv \max_{\kappa \neq 0} g(t). \quad (13)$$

In a linearly stable situation, the quantity $G(t)$ increases initially, and after attaining a maximum G_{max} , decays to zero as $t \rightarrow \infty$. For a given value of Re, α, β and θ , G_{max} is thus the maximum possible factor over which the initial disturbance kinetic energy can grow algebraically. Our computations of $G(t)$ for a plane channel at Reynolds numbers of 1000 and 1500 (appropriately scaled) at different Knudsen numbers are, as mentioned above, in excellent agreement with [2] and [1] respectively.

The contours of constant G_{max} for a range of α and β are plotted in Figure 11 for a Reynolds number of 200 and wall slopes of 0.005 and 0.02. The solid line represents the G_{max} at $Re = 200$ for $Kn = 0.0$, whereas the dashed line represents $Kn = 0.1$. It is evident that velocity slip as well as channel divergence have only a marginal effect. We now define a Reynolds number $Re_{0.95}$ equal to 95% of the linear

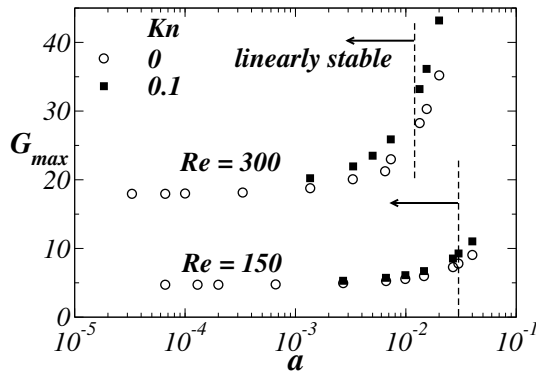


Fig. 12. The maximum transient growth of disturbance kinetic energy at $\alpha = 0$, $\beta = 2.0$ as a function of slope. The vertical lines show the divergence beyond which the flow is linearly unstable at each Reynolds number.

instability-critical Reynolds number Re_{cr} for that particular angle of divergence. The algebraic amplification of disturbances obtained at this Reynolds number is close to the maximum possible, since exponential growth will take over at a higher Reynolds number for that angle of divergence. The Reynolds number of 200 at which the contours are shown is about two-fifths of Re_{cr} at $a = 0.005$, while at $a = 0.02$, $Re_{0.95} = 200$. The point to be stressed here is that, even at this “high” Re for $a = 0.02$, the growth is comparable with that of $a = 0.005$. The maximum algebraic growth (i.e., the maximum contour value in Fig. 11) obtained just before linear instability serves only to amplify the initial perturbation by a factor of ~ 15 . This is in contrast to a plane channel, where the factor is about 200 even at one-sixth of Re_{cr} [17]. The results are qualitatively the same over a range of Re and θ .

Throughout the Knudsen number range considered here, the largest transient growth is obtained for streamwise independent disturbances ($\alpha = 0$) of spanwise wavenumber β close to 2, so the remaining results are presented at these wavenumbers. It should be stressed here that the comparisons made are valid irrespective of α and β . Figure 12 shows the G_{max} at Reynolds numbers of 150 and 300. The slope at which the flow becomes linearly unstable (to two-dimensional perturbations) is shown by the vertical line in each case. The values of $G_{max}(\alpha = 0, \beta = 2)$ shown beyond this point correspond to the first local maximum. Although this value sharply increases with divergence, it has been checked to be irrelevant in comparison to the exponential growth in the two-dimensional mode. In the linearly stable range, transient growth is (i) small, and (ii) relatively insensitive to wall divergence, unlike the dominant linear mode, which is hugely destabilised. The small destabilising effect of slip on transient growth is summarised in Figure 13. The combination of wall divergence and wall slip on plane channel is, thus shown to have insignificant algebraic growth. We may conclude that the algebraic growth mechanism is not a major player in diverging channels, whether with or without slip.

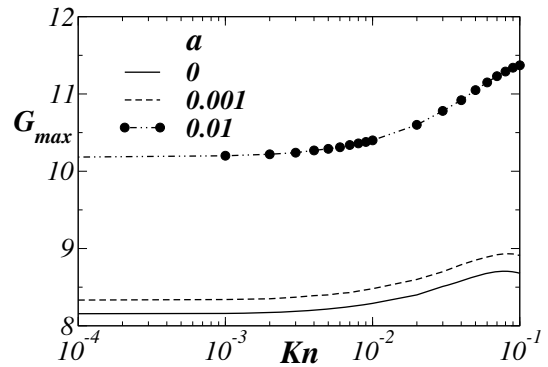


Fig. 13. The maximum transient growth of disturbance kinetic energy at $\alpha = 0$, $\beta = 2.0$ as a function of Knudsen number. The Reynolds number in is 200.

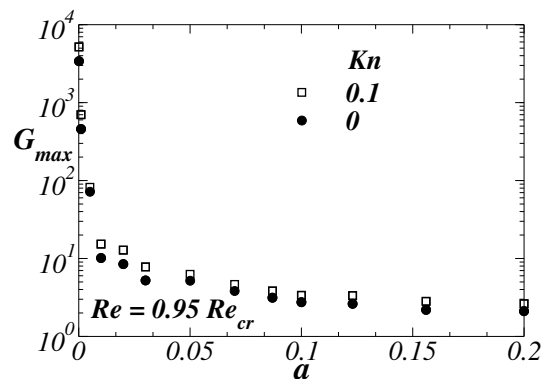


Fig. 14. G_{max} at $\alpha = 0$ and $\beta = 2$, as a function of wall divergence at $Re_{0.95}$. The point at the lowest slope ($a = 10^{-4}$) is obtained at a Reynolds number of $Re_{0.95} = 4282$, while at $a = 0.2$, $Re_{0.95} = 56.6$.

In Figure 14, it is seen that the transient growth obtainable just below Re_{cr} (i.e., $Re_{0.95}$) drops sharply with wall divergence, and is very small even for modest divergence. This result is compared to the maximum transient growth in a plane channel in Figure 15, solid line. Note that the dashed lines in this figure consist of points from Figure 14 obtained at various levels of wall divergence, each at its $Re_{0.95}$. At values of wall divergence below 2 degrees or so, the two lines without slip are almost indistinguishable, showing that G_{max} is primarily dependent on the Reynolds number and not on the slope. Scaling arguments at small α show [17] that G_{max} should vary as Re^2 . This has been shown to hold true for a variety of flows such as for plane Poiseuille, plane Couette, flow in circular pipes and Blasius boundary layers, with different constants of proportionality. The relationship is seen to hold in the case of divergent flows as well, with $G_{max} \sim f(Kn)Re^2$ where $f(Kn)$ is a weak function of Kn . At higher divergences, where the velocity profile is close to separation at the wall, there is a clear deviation from the power law. This could be of theoretical interest, and merits further investigation.

For the streamwise-independent modes ($\alpha = 0$) our finding that the velocity profile, and thus the level of divergence, do not affect the transient growth, are consistent

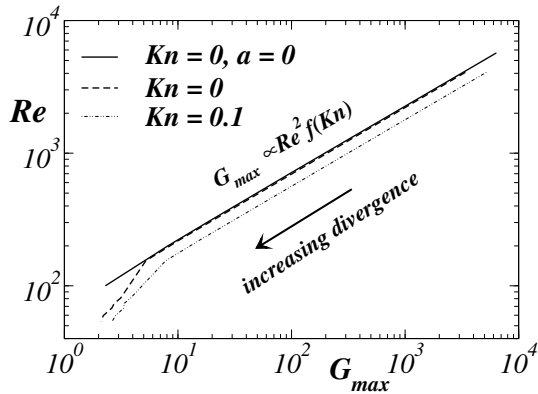


Fig. 15. G_{max} at $\alpha = 0$ and $\beta = 2$, as a function of Reynolds number. The solid line is for a plane channel without slip. The long dashes are the quantity shown in 14 plotted now against $Re_{0.95}$. The coincidence of the two lines over most of the range shows that unlike linear instability, the transient growth is not affected by wall slope. The power law behaviour is seen to hold for slip flow as well.

with earlier analyses on boundary layers [17,18]. However, at this point we do not have an analytical explanation for the insensitivity to divergence. Note that the Orr-Sommerfeld and Squire equations reduce in this case to

$$\frac{1}{Re} \left(\frac{\partial^4 v}{\partial y^4} - 2\beta^2 \frac{\partial^2 v}{\partial y^2} + \beta^4 v \right) = \omega_i \left(\frac{\partial^2 v}{\partial y^2} - \beta^2 v \right), \quad (14)$$

$$\omega_i \eta + \frac{1}{Re} \left(\beta^2 \eta - \frac{\partial^2 \eta}{\partial y^2} \right) = -i\beta U' v. \quad (15)$$

$\hat{\eta}$ is the y component of disturbance vorticity whose amplitude η is defined as in equation (5), and $\omega = i\omega_i$, since $\omega_r = 0$ for $\alpha = 0$. v is now independent of the velocity profile, but η is not.

For $Kn > 0.1$ we find that the nature, and level of stabilisation is different, but since the slip model is no longer appropriate here, this range is being approached in a different study.

To summarise, it is known that in a plane channel, at Reynolds numbers of about a quarter of Re_{cr} , the levels of transient growth are so high that they can trigger nonlinearities and a transition to turbulence (see e.g. [18]). Recent work shows that a velocity slip at the wall (for small Knudsen numbers) does not much affect transient growth. The implication is that, were the channel to be perfectly plane, one would not expect any big difference in the route to transition, with or without slip. Here, we have investigated how two opposing sources of linear instability affect channel flow. We show that for small divergences of the channel wall, the transient algebraic growth is an insignificant player, whether or not the flow is slipping at the wall. Linear instability on the other hand occurs at Reynolds number two orders of magnitude

lower than in a plane channel in spite of the presence of wall slip. We predict that in the presence of divergence and slip, route to chaos is via linear instability for channel and hope to motivate experimental verification of this assertion. We thus expect that in the presence of local divergence a finite amplitude growth of disturbance will lead to turbulence, irrespective of background noise or slip.

We have considered only Jeffery-Hamel flows, representing long channels with constant divergences, but our results are relevant to channels of arbitrary geometry with local divergences extending to a few channel widths. We have checked that numerical profiles obtained in such channels match closely with Jeffery-Hamel profiles. Restricting ourselves to situations where the inlet flow is relatively quiet, we have not touched upon the role of non-linearity here, but there are several interesting questions, such as whether a nonlinear self-sustaining mechanism of the general class of [19] would be in operation or whether nonlinear traveling-wave solutions [20,21] will be observed.

We acknowledge financial support from the Defence R&D Organisation, Government of India.

References

1. E. Lauga, C. Cossu, *Phys. Fluids* **17**, 088106 (2005)
2. T. Min, J. Kim, *Phys. Fluids* **17**, 108106 (2005)
3. C. Gan, Z. Wu, *J. Fluid Mech.* **550**, 289 (2006)
4. P.M. Eagles, *J. Fluid Mech.* **24**, 191 (1965)
5. P.M. Eagles, M.A. Weissman, *J. Fluid Mech.* **69**, 241 (1975)
6. K.C. Sahu, R. Govindarajan, *J. Fluid Mech.* **531**, 325 (2005)
7. J.C. Maxwell, *Phil. Trans. Roy. Soc. Lond.* **170**, 231 (1879)
8. E.S. Piekos, K.S. Breuer, *J. Fluids Eng.* **118**, 464 (1996)
9. A.K.H. Chu, *Europhys. Lett.* **64**, 435 (2003)
10. A.K.H. Chu, *J. Phys. Condens. Matter* **12**, 8065 (2000)
11. A.K.H. Chu, *Comptes Rendus Mécanique* **332**, 895 (2004)
12. J.M. Gersting, *Phys. Fluids* **17**, 2126 (1974)
13. L. Rayleigh, *Proc. London Math. Soc.* **11**, 57 (1880)
14. P.G. Drazin, W.H. Reid, *Hydrodynamic Stability* (Cambridge University Press, Cambridge, 1981), pp. 153-164
15. F.P. Bertolotti, T. Herbert, P.R. Spalart, *J. Fluid Mech.* **242**, 441 (1992)
16. K.C. Sahu, Ph.D. thesis, Jawaharlal Nehru Centre for Advanced Scientific Research, Bangalore, India, 2006
17. P.J. Schmid, D.S. Henningson, *Stability and Transition in Shear Flows* (Springer-Verlag, New York, 2001)
18. W.O. Criminale, T.L. Jackson, D.G. Lasseigne, R.D. Joslin, *J. Fluid Mech.* **339**, 55 (1997)
19. F. Waleffe, *Stud. Appl. Math.* **95**, 319 (1995)
20. B. Hof, C.W.H. van Doorne, J. Westerweel, F.T.M. Nieuwstadt, H. Faisst, B. Eckhardt, H. Wedin, R.R. Kerswell, F. Waleffe, *Science* **305**, 1594 (2004)
21. H. Faisst, B. Eckhardt, *J. Fluid Mech.* **504**, 343 (2004)